Renewable and Sustainable Energy Reviews 33 (2014) 412–426

Contents lists available at ScienceDirect

Renewable and Sustainable Energy Reviews

journal homepage: www.elsevier.com/locate/rser

Reconfigurable electrical interconnection strategies for photovoltaic arrays: A review

Damiano La Manna, Vincenzo Li Vigni, Eleonora Riva Sanseverino *, Vincenzo Di Dio, Pietro Romano

DEIM, University of Palermo, Palermo, Italy

ARTICLE INFO

Article history:
Received 26 June 2013
Received in revised form
27 December 2013
Accepted 29 January 2014
Available online 5 March 2014

Keywords:
Partial shading
Reconfigurable photovoltaic array
Electrical mismatch
Reconfiguration algorithm
TCT
Switching matrix
MPPT

ABSTRACT

Non-uniform irradiance significantly decreases the power delivered by solar photovoltaic arrays. A promising technique for compensating these power losses relies on dynamically reconfiguring the electrical connections between photovoltaic modules. This paper presents the current state-of-the-art strategies for photovoltaic array reconfiguration in order to increase the power output under partial shading and mismatch conditions. The different approaches have been compared in terms of effectiveness of the control algorithms, monitored electrical and environmental variables, overall hardware complexity and specific features of each solution. Finally, the most challenging aspects of the reconfiguration strategy are identified and further discussed.

Contents

1. Introduction

Electrical energy production from renewable sources gained strong importance in the last two decades due to many reasons. First and most important of all, the political framework; EU directives are now supporting the energy production from renewables such as the 20–20–20 directives [1] and, as a consequence, many national governments are encouraging the adoption of renewable energies providing financial incentives [2]. Secondarily, the virtually unlimited availability of energy from natural

* Corresponding author.
E-mail addresses: damiano.lamanna@unipa.it (D. La Manna), vincenzo.livigni@unipa.it (V. Li Vigni), eleonora.rivasanseverino@unipa.it (E. Riva Sanseverino), vincenzo.didio@unipa.it (V. Di Dio), pietro.romano@unipa.it (P. Romano).

http://dx.doi.org/10.1016/j.rser.2014.01.070
1364-0321

Nomenclature

A	ideality factor of a solar cell
BIPV	building integrated photovoltaic system
BL	bridge linked
COI	configurations of interest
DAQ	data acquisition system
DES	dynamic electrical Scheme
DPST	double-pole single-throw switch
EAR	electrical array configuration
EI	equalization index
G	irradiance
HC	honey-comb
i	row index
I–V	current–voltage
I_0	module reverse-bias diode saturation current (A)
I_L	light-generated current
I_{sc}	module's short circuit current
j	column index
k	Boltzmann's constant
m	number of rows
MPP	maximum power point
MPPT	MPPT Maximum power point tracker
n	number of columns
N_{PV}	number of photovoltaic modules
Ns	module's total number of series cells
NSW	number of switches
P–V	power–voltage
PV	photovoltaic
q	electron charge
R_s	module's series resistance
R_{sh}	shunt resistance of a solar cell
SP	module's series resistance
SPDT	single-pole double-throws switch
SPST	single-pole single-throw switch
STC	standard test conditions
T_c	operating temperature
TCT	total cross tied
V_{oc}	open-circuit voltage
V_t	module's thermal voltage (V)

resources and, in particular, the energy harvested from the solar source represents one of the most exploited solutions thanks to the development of efficient technologies for Photovoltaic (PV) generation [3]. In Fig. 1, the generic layout of a PV generation system is shown. The PV plant includes a set of PV arrays and the conversion group interfacing the arrays to the power grid. Each PV array is composed of a number of parallel connected PV strings, Series Parallel, SP, topology, or of a number of series connected tiers, Total Cross Tied, TCT, topology. In Fig. 1 a PV plant with SP topology is reported.

Nonetheless, the use of this source through PV array generators is affected by specific limits caused by the low efficiency-per-m^2 of conversion devices [4,5], the discontinuity of the solar source due to the alternating day and night, the high cost/kW-produced ratio, the unpredictability of weather conditions and finally the not efficient working conditions due to electrical mismatch. As it will be detailed in the following sections, differences in electric characteristics between solar cells composing a single PV module and between PV modules composing a PV string lead to a strong reduction of the output power of the whole PV plant [6,7].

All the above factors create a gap between the potential energy production and the actual energy extracted. Nowadays, the scientific community is further improving the conversion efficiency of PV modules [8–11] reducing costs per kW as well as implementing new and efficient algorithms for power conversion electronic devices interfacing the PV generator to the AC section, Maximum Power Point Tracking (MPPT) algorithms [12–14]. These algorithms are implemented in the power conversion group controller and let the PV array output the maximum power, by forcing the input impedance of the conversion group to match the maximum power operating point of the PV array.

Other interesting research fields trying to overcome the cited limits are solar tracking strategies [15] and efficient faults detection algorithms [16,17].

A leading-edge research area is developing *dynamic reconfiguration strategies*, namely efficient ways to dynamically change the connection layout of PV modules into PV arrays in order to improve power output under electrical mismatch conditions caused by partial shading and other issues. For instance, when one or more series-connected PV modules are shaded, the maximum permitted current is reduced, consequently decreasing the power output [18]. Moreover, the shaded or faulty module can reach critical high temperature, leading to the hotspot phenomenon [19–23] and consequently to the failure of the module. Bypass diodes avoid the hotspot and mismatch events [24,25], but they introduce losses and local maxima in the electrical characteristics of the PV module [26].

The MPPT algorithm implemented for the inverter control can be misled and the local maximum operating point can be

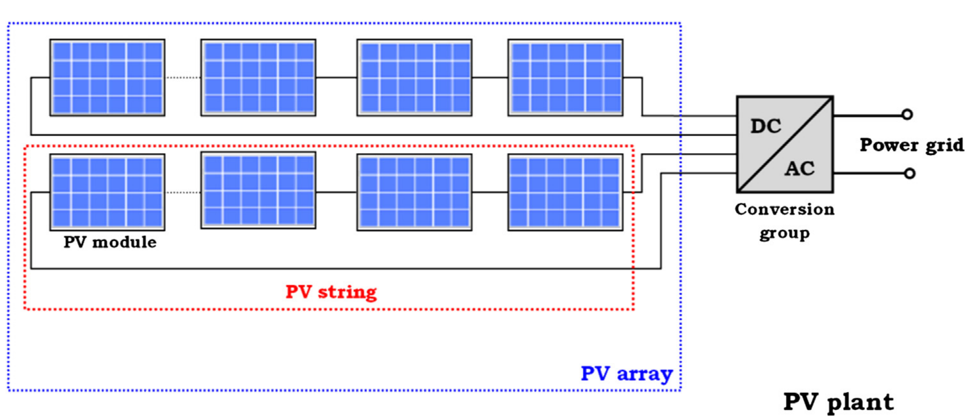


Fig. 1. PV plant components: series connected modules form a PV string, more parallel connected strings form a PV array. A PV plant includes also the conversion group transferring energy to thepower grid.

considered as absolute maximum [27]. As a result, the PV array would not produce the maximum output power. For these reasons, new smart strategies have been developed to find the absolute maxima of P–V curves [28–30].

Micro-inverter architecture [31,32], as well as dynamic reconfiguration strategies may increase the energy production of the PV plant, limiting electrical mismatch issues. The Micro-inverter architecture for the power conversion group has been recently proposed together with interesting solutions to locally adapt the P–V curve of the PV module to the maximum operating point as it will be detailed in Section 2.3.

Dynamic reconfiguration strategy can be applied to different target applications. The first case is when the plant is affected by the shadow projected by a fixed object. This is common for PV plants placed on roofs or integrated in buildings. As an example, in [33,34] the dynamic reconfiguration approach has been applied to Building Integrated Photovoltaic Systems (BIPV). BIPVs are of great interests since they enable to take advantage of wide areas exposed to sunlight offered by buildings.

The second case is when a portion of a large PV plant is affected by passing clouds. In this case there is generally a distributed drop of the irradiance above all the PV plant. Depending on the speed of the clouds producing a shade on the PV plant, the irradiance conditions can change suddenly, giving rise to a large deterioration of the PV plant efficiency that may last a long time, thus producing a reduction of the energy generated by the solar source. Finally, in the event of failure of one or many solar modules, these can be automatically disconnected by the reconfigurable array.

The design of dynamic reconfiguration systems that can cope with environmentally variable conditions, shadings or failures both in small as well as in larger plants is influenced by many challenging aspects, influencing the control chain as depicted in Fig. 2.

The *data acquisition* is performed through suitable measurement devices allowing to collect the field data required for the *PV mathematical model* providing input data for the *reconfiguration algorithm*. The latter two compose an open loop control system and thus the more accurate the PV mathematical model, the best control actions the reconfiguration system will give to the actuator. The *switching matrix* is the actuator. It implements the desired *optimal configuration of the PV plant* . In the following sections each of the cited elements of the control chain will be detailed.

In this paper, a review on the state-of-the-art research on PV reconfiguration strategies to improve power output under non-uniform shading conditions is presented. Two interconnection topologies have been identified as the most interesting in the reported reconfiguration systems: Series-Parallel (SP) and Total-cross-tied (TCT). These two categories have been adopted in this work to classify the different approaches. These have been compared in terms of effectiveness of the control algorithms, monitored electrical and environmental variables, overall hardware complexity and specific characteristics of each solution, further focusing on the most challenging aspects of any reconfiguration approach.

The work is thus organized as follows. In Section 2 the most relevant general issues about the reconfiguration strategy are outlined. The electrical mismatch issue is first considered in Section 2.1. with a focus on the partial shading problem. Then the different architectures of the power conversion system are outlined in 2.2., where their main features with reference to the mismatch issue are discussed in each case. Finally, a deeper insight about the PV mathematical model is presented in Section 2.3.

2. General issues

2.1. Electrical mismatch and partial shading

Differences in electric characteristics of solar cells lead to mismatch losses [35,36] inside the module, while modules with different electrical characteristics lead to mismatch in the whole PV plant [6]. Both issues can be influenced by factors that are internal or external to the module. Internal factors include non-homogeneous characteristics of solar cells, caused by manufacturing defects, faulty solar cells and malfunction of one PV module [37]. External factors include degradation of materials used to encapsulate the cells, dirt deposited on the cell surface, different temperatures [38] and shading [39]. In particular, partial shading of PV modules occurs when these are subjected to passing clouds, smog layer or common urban elements such as chimneys, electricity pylons and surrounding buildings and dirt. The nature of dirt is also strictly related to the location where the PV plant is installed, for instance, ashes can be present near volcanic areas and salt deposits might be found by the seaside. All these factors lead to a reduction of the module performances, implying that the generated power of a PV plant is less than the sum of the generated power of each solar module when working as stand-alone.

When modules with different electrical characteristics are connected in a PV array [40], the mismatch issues become critical. In fact, the solar module in the worst operating condition determines the output current of the entire series-connection, leading also to non-recoverable reverse bias breakdown, hotspot phenomena and excessive power depletion as a result of mismatch effects [19] [41–43].

Since mitigation of mismatch losses in a solar array is always necessary, most commercial PV modules incorporate one or more bypass diodes, inserted in parallel to a group of cells series-connected [25] [44]. The presence of bypass diodes significantly affects the electrical curves of the PV array and creates one or more local maximum power points (MPP) in the P–V characteristic when a significant mismatch occurs, see Fig. 3.

Therefore, distortion of shaded I–V curve may lead to an error in the determination of the global MPP[42]. In the literature, some efficient simulation tools have been described [45–47].

2.2. Power conversion architecture

For grid-connected PV plants a proper design of the architecture of the power conversion group is required. The choice of the number of inverters and their configuration affects significantly the performance, reliability, mismatch rejection and of course costs of the plant. Many architectures for the PV generator have been adopted in real-world cases. The most commonly reported architectures are [48–50]:

1. Central-inverter architecture (Fig. 4a): all the strings are connected to the input of the common unique inverter, thus implementing the MPPT for the whole array. This solution is

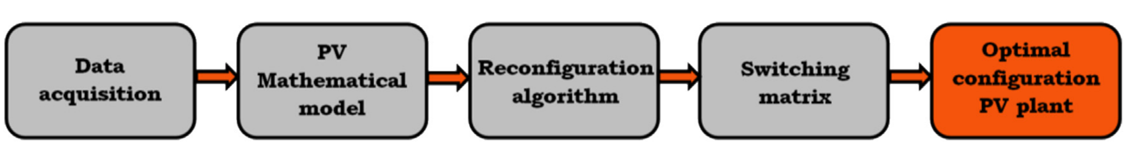


Fig. 2. Dynamic reconfiguration system for PV plant: flow chart for optimal operation.

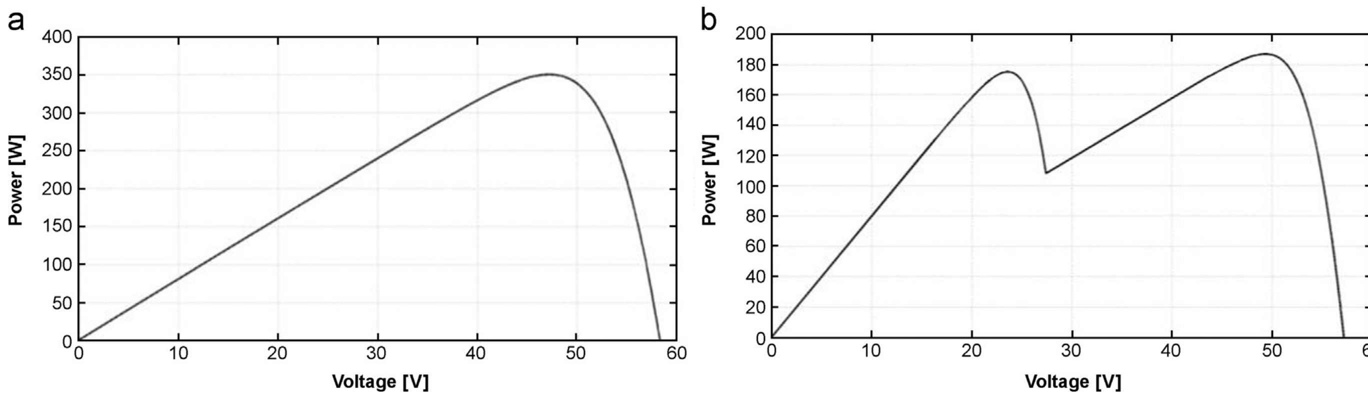


Fig. 3. Effects of mismatch condition in P–V curve, in particular: (a) typically P–V curve for PV module in standard condition with single maximum, (b) P–V curve with two local maxima.

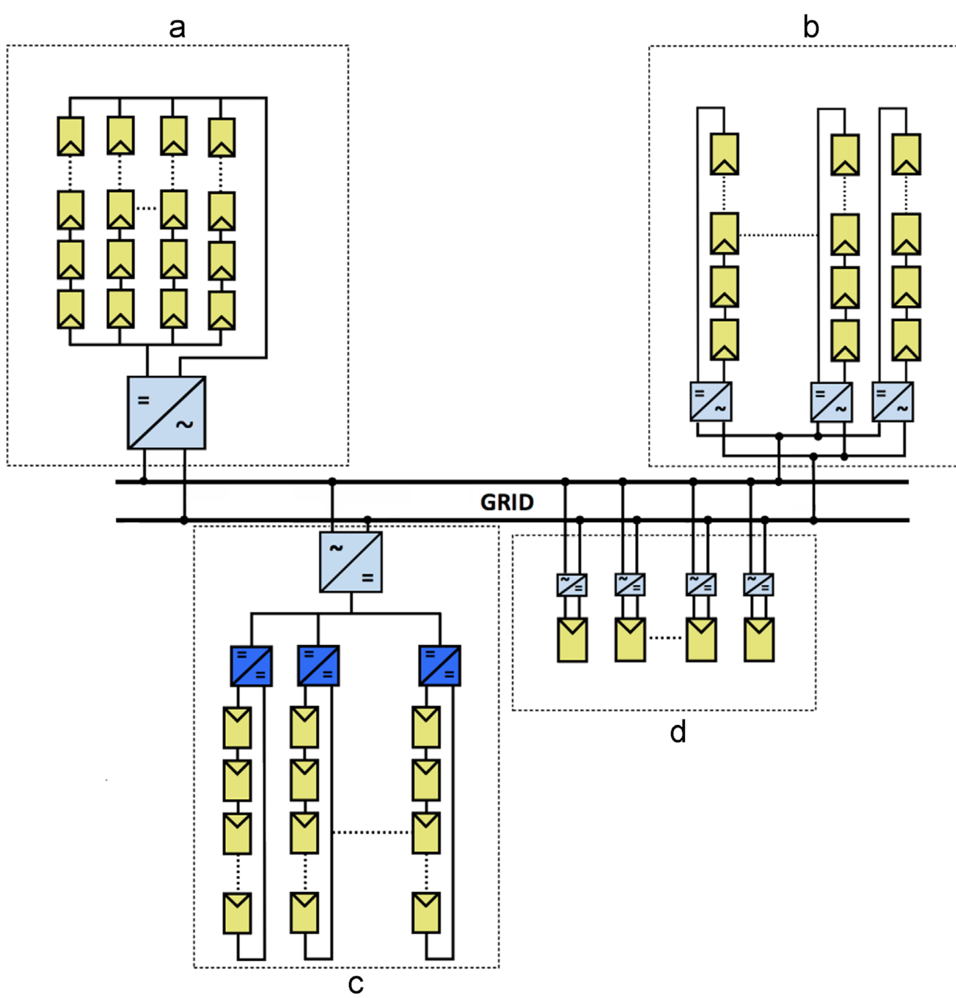


Fig. 4. PV generator architecture: (a) Central inverter, (b) String inverter, (c) Multi-string inverter architecture, (d) Micro-inverter architecture.

usually simpler and cheaper but has the disadvantage that mismatch losses are higher. These can be compensated by means of a reconfigurable interconnection array.

2. String-inverter architecture (Fig. 4b): every string has its own inverter thus performances under partial shading condition are increased. Usually this is the case when an inverter presenting more MPPT input channels is used, where each is generally a stand-alone inverter itself implementing its own MPPT algorithm. In this case, a reconfiguration approach could create strings by connecting solar modules with similar irradiance levels. Namely, solar modules are exchanged between strings, thus increasing the over power output.[49].
3. Multi-string inverter architecture (Fig. 4c): a DC/DC boost converter is installed in each string. All the DC/DC outputs insist on a common DC bus and this is finally connected to the DC/AC stage. This solution combines both the advantages

of the cheaper central-inverter architecture and the better performances of the string-inverter architecture. Even in this case, a reconfiguration approach creates strings by connecting solar modules with similar irradiance levels.

4. Micro-inverter architecture (Fig. 4d): each module has its own inverter with a dedicated MPPT and all the micro-inverter outputs are connected to a unique AC bus [51]. PV plants adopting this solution are ideally immune from mismatch losses caused by different irradiance degrees and thus the reconfigurable approach does not apply. The disadvantages are essentially higher costs of each micro-inverter [52]. Moreover they may show a more limited reliability since they are exposed to varying weather conditions (i.e. rain, snow). In fact, the single inverter of the first solution is usually stored in a proper housing providing more stable environmental conditions [53,54].

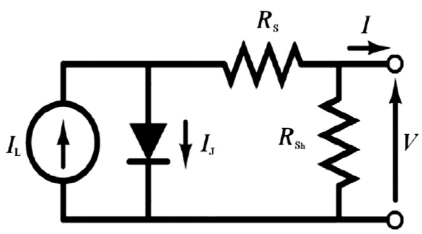


Fig. 5. Circuit of the 5-parameter model of a photovoltaic cell.

In Section 3, the most interesting reconfiguration strategies that can be implemented over different existing PV plants topologies proposed in the literature are presented.

2.3. Mathematical model of PV cells

As discussed in Section 1, dynamic reconfiguration strategy depends on a good modelling of the PV array. Infact, the best choice of the mathematical model is necessary for the optimal design and simulation of the PV array under partial shading conditions. A PV module mathematical model is built starting from the solar cell model. In the literature, many different models to describe the solar cell have been proposed [55–59]. Depending on the number of the parameters used to model the solar cell [60–66], the accuracy improves while their implementation [46] and the computational complexity are increased. A good compromise between accuracy and calculation times, compatible with an elaboration over a microcontroller, is a 5-parameter model [67,68]. The circuit model is shown in Fig. 5 .

For a module composed of many solar cells series-connected, the total module current I is expressed by

$$I = I_L - I_0\left(e^{\frac{V+IR_s}{N_s A V_t}} - 1\right) - \frac{V+IR_s}{R_{sh}} \quad (1)$$

where I_L is the light-generated current, I_0 the diode reverse saturation current, R_s and R_{sh} respectively the cell series and shunt resistance, N_s the number of cells series-connected, A the ideality factor and $V_t = kT_c/q$, with k the Boltzmann's constant and q the

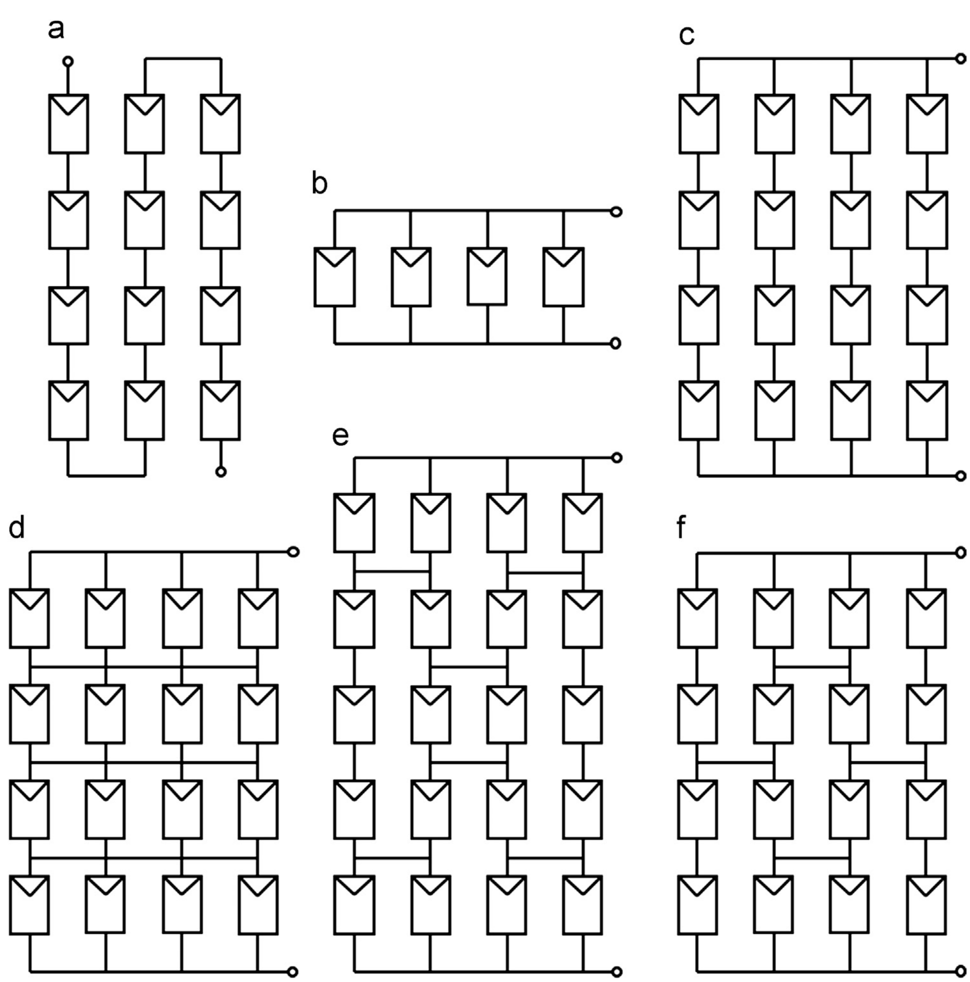


Fig. 6. Connection topologies of the PV array. (a) Series array, (b) parallel array, (c) series-parallel array, (d) total-cross tied array, (e) bridge-link array and (f) honey-comb array.

electron charge and T_c the temperature of cell. It is worth noticing that (1) is a transcendental equation and parameters have to be quantified considering their dependence on solar radiation and temperature [38] [69]. In particular, while the ideality factor A is a constant value that does not vary with temperature (its value measure the junction quality and the type of recombination in a solar cell) [69], I_0, I_L, are temperature-dependent, as depicted in

$$I_0 = I_{d0}\left(\frac{T_c}{T_{C_{STC}}}\right)^3 \exp\left[\frac{qE_g}{Ak}\left(\frac{1}{T_{C_{STC}}}-\frac{1}{T_c}\right)\right] \quad (2)$$

where I_{d0} is the reverse saturation current in STC and E_g is the band gap energy in (eV):

$$E_g = 1.16 - 7.02\times10^{-4}\frac{{T_c}^2}{T_c+1108} \quad (3)$$

The light-generated current can be expressed by

$$I_L = \left(\frac{G}{G_{STC}}\right)[I_{L_{STC}} + \mu_{1_{SC}}(T_c - T_{C_{STC}})] \quad (4)$$

where G is the solar radiation measured in W/m^2, G_{STC} the solar radiation in standard conditions, STC, (1000 W/m^2), $T_{C_{STC}}$ the temperature at STC (298,15 K),$\mu_{1_{SC}}$ is the short-circuit current temperature coefficient. $I_{L_{STC}}$ is the PV cell light-generated current at STC. R_s and R_{sh} represent the energy losses and voltage drops occurring in the presence of the photocurrent [70–73]. There are two approaches to calculate the model parameters: one is numerical, in which the parameters are calculated iteratively and the second involves the extraction of the parameters analytically [46] [74,75].

Table 1
Summary of Velasco et al. approach [88].

Reconfiguration strategy	Irradiance equalization
Control algorithm	–
Number of switches	2 N_{PV} m- throws
Acquired parameters	Voltage and current of the module
Complexity	Medium

Substituting (4) in (1), the following expression is obtained:

$$G = \frac{G_{STC}}{I_{L_{STC}} + \mu_{1_{SC}}(T_c - T_{C_{STC}})}\left[I + I_0\left(e^{\frac{V+IR_s}{N_sAk\frac{T_c}{q}}} - 1\right) + \frac{V+IR_s}{R_{sh}}\right] \quad (5)$$

Eq. (5) provides an accurate way to estimate the solar radiation received by the PV module by measuring its voltage, current and temperature, provided that all the other terms in (5) are fixed. Furthermore, the solar radiation can be estimated even with two parameters only, one of which is the temperature, in the following two cases:

(a) the solar module can be put in open-circuit and the V_{oc} acquired, as in [76];
(b) the solar module can be put in short-circuit and the I_{sc} acquired, as in [77];

In the two cases, the solar radiation is respectively given by

$$G = G_{STC}\, e^{\frac{V_{oc} - V_{oc_{STC}} - \mu_{V_{oc}}(T_c - T_{c_{STC}})}{N_sAk\frac{T_c}{q}}} \quad (6)$$

$$G = \frac{G_{STC}}{I_{SC_{STC}}}(I_{sc} - \mu_{I_{sc}}(T_c - T_{c_{STC}})) \quad (7)$$

where $\mu_{V_{oc}}$ is the open-circuit voltage temperature coefficient and $I_{SC_{STC}}$ the short-circuit current in STC.

Eqs. (5), (6) and (7) represent three different strategies for estimation of irradiances, namely the necessary inputs of the algorithm controlling the dynamic reconfiguration system.

Indeed from the diagnosis of the working conditions of the modules, that can be carried out based on the above considerations, rather than on costly measures, the reconfiguration algorithm can identify the best PV plant configuration.

3. Reconfiguration strategies

In the literature, many alternative array interconnection topologies have been proposed for reducing mismatch losses [78–84]. Series and parallel topologies, Fig. 6 a and b, are the basic configurations, with the main disadvantages that, respectively,

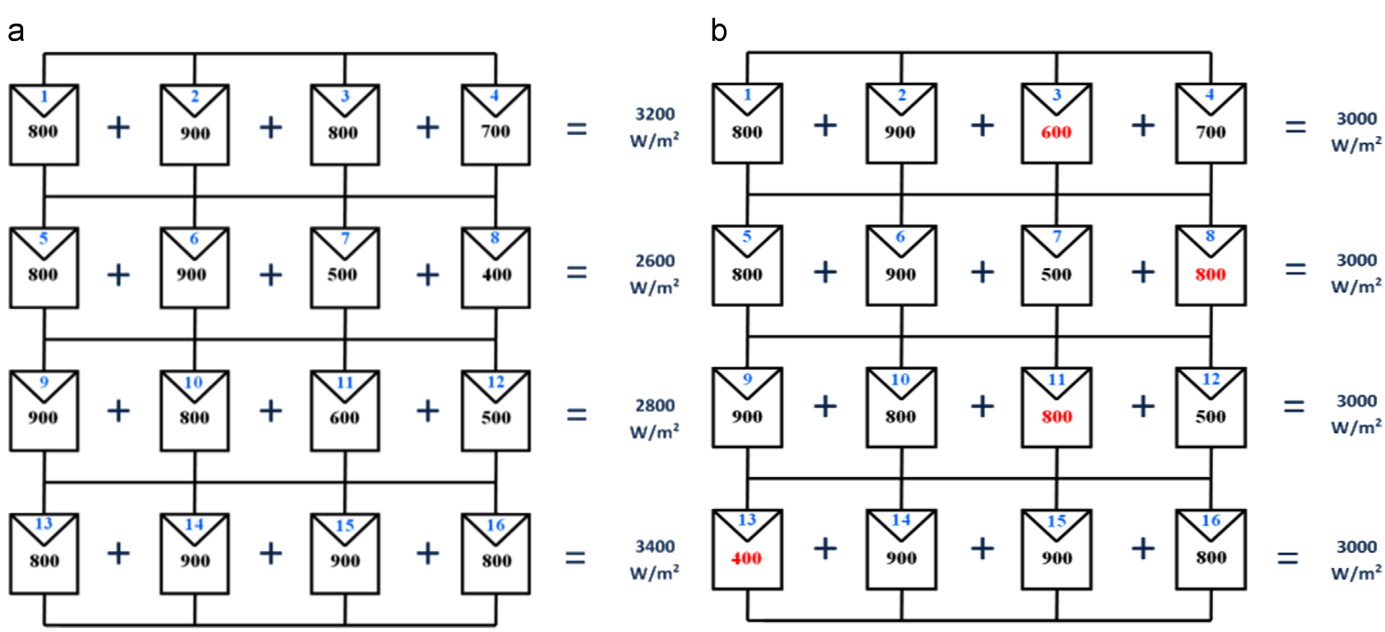


Fig. 7. Irradiance equalization example: (a) before sorting, rows have different irradiance levels: 3200, 2600, 2800 and 3400 W/m^2; (b) changing PV modules position following a reconfiguration approach (modules 3–11 and 8–13 have been switched, the irradiance could be equalized as 3000 W/m^2.

the current and the voltage are below the practical desired values. During partial shading, parallel-connected PV elements produce higher power than series-connected ones, since in the parallel connection the overall current is the summation of all the currents [22] and voltages do not vary very significantly[85]. However, higher currents flow in parallel-connected elements, so that power losses[86] and voltage drops are generally higher and cabling is more expensive. In actual PV power plants, the serial-parallel (SP) is the most common connection. It is obtained connecting solar modules in series to form a string (necessary to reach the voltage required by inverter input ranges); strings are then connected in parallel to increase the total current (as shown in Fig. 6c). In Total-cross-tied (TCT) configurations (see Fig. 6d), modules are first parallel tied so that voltages are equal and currents are summed up; many of these groups are then connected in series. Though under uniform conditions SP and TCT modules connection provide the same power value, the TCT topology reduces the overall effect of mismatch. In the Bridge-link (BL) topology, in Fig. 6e, about half of the interconnections of the TCT topology are avoided, so that cable losses and wiring installation time are reduced [87]. Though, in larger installations the TCT arrangement can be easier to wire because of the simplicity of the pattern [78]. Advantages shown by both TCT and BL topologies have been combined in the Honey-Comb (HC) configuration (in Fig. 6f).

Although many convenient interconnection topologies have been developed, so far the most exploited solutions rely on TCT and SP module interconnections.

In the following sections, the different reconfiguration approaches proposed in the literature have been compared in terms of effectiveness of the control algorithms, monitored electrical and environmental variables, overall hardware complexity and specific characteristics of each solution, further focusing on the most challenging aspects of a reconfiguration approach. In each approach the hardware implementation is also considered by means of the evaluation of the number of required switches. In Section 4.2, the issue is more extensively treated.

3.1. Reconfiguration for TCT topology

As already discussed in this work, the TCT interconnection allows to reduce the overall effects of mismatch. The challenge in a TCT reconfiguration technique consists in connecting PV modules in irradiance-balanced tiers. An interesting optimization algorithm based on the use of an equalization index was presented in [88]. As it will be detailed right below in this section, *irradiance equalization* aims to obtain series connected tiers, also called rows, where the sum of the irradiances of the modules is the same; this

Table 2
Summary of Romano et al. approach [91].

Reconfiguration strategy	Irradiance equalization
Control algorithm	Deterministic and random search
Number of switches	$N_{sw} = (2mN_{Pv})_{DPST} + (m)_{SPDT}$
Acquired parameters	Voltage and current of the module
Complexity	Medium

Table 3
Summary of Wilson et al. approach [92].

Reconfiguration strategy	Irradiance equalization
Control algorithm	Best worst sorting
Number of switches	$N_{SW} = N_{PV}(m^2 - m)$
Acquired parameters	Voltage and current
Complexity	Medium – High

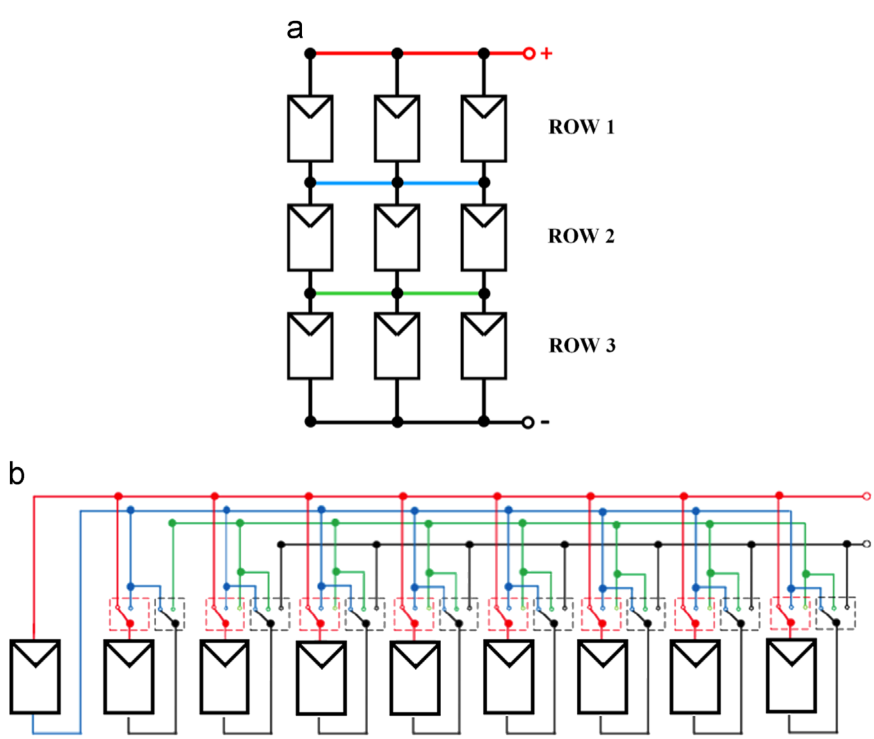


Fig. 8. (a) Electrical scheme for a square switching matrix $m=n=3$. (b) Every module is connected to the electrical bus with m-throw switches. In particular, the position of the first module in the matrix is fixed to the row one, the second could be connected to the first or second row. The others may be connected indifferently to the first, second or third row.

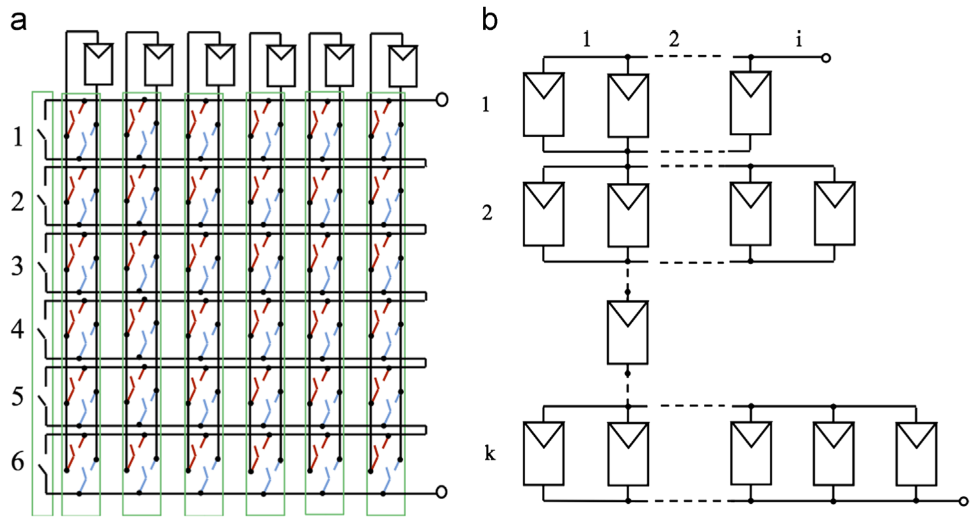


Fig. 9. DES structure for 6 modules (a) and non symmetric matrix (b).

Table 4
Summary of Nguyen et al. approach [76].

Reconfiguration strategy	Adaptive bank
Control algorithm	Bubble sort and model based
Number of switches	$(2N_{AB}N_{PV})SPST$
Acquired parameters	Operating and open circuit voltage, temperature
Complexity	Medium

results in a string where the circulating current is proportional to the given sum of irradiances of one row. The algorithm equalizes the available power on each row, thus n ideal current generators, with the same nominal values, are connected in the string, avoiding mismatch losses.

Indicating with G_{ij} the irradiance value of the module located on row I and column j within the topology showed in Fig. 7, the total irradiance of the row i is defined as

$$G_i = \frac{\sum_{j=1}^{m} G_{ij}}{m} \tag{8}$$

where m is the number of modules that are parallel connected.

For each configuration, the algorithm calculates the equalization index (EI) by means of the following expression:

$$EI = \max_i(G_i) - \min_i(G_i) \forall i \tag{9}$$

This index quantifies the degree of current limitation of the configuration and thus the one minimizing EI is selected. The secondary aim pursued by the algorithm is the smallest number of switching operations starting from the initial configuration. Under the same equalization index, the configuration with the least number of switching operations to be performed is selected.

In [89] a PV generator with an electrical array configuration (EAR) controlled by the irradiance equalization algorithm has been presented. The EAR PV generator is composed of a static part, necessary to meet the input range constraints of the inverter, and a reconfigurable one, controlled by the irradiance equalization algorithm.

Although all the possible interconnections of PV modules are $(m \cdot n)!$, the total configurations of interest (C), namely the configurations delivering different values of output power, are

$$C = \frac{(m \cdot n)!}{m! \cdot (n!)^n} \tag{10}$$

with m and n the number of rows and columns.

All the configurations of interest can be achieved by using a number of switches, N_{sw}, equal to

$$N_{sw} = 2N_{PV} \tag{11}$$

These N_{sw} switches are of single-pole m-throws type and N_{PV} is the number of PV modules. It should be noted that, if not commercially available, it is necessary to emulate a m-throw switch by connecting m single pole switches in parallel, thus increasing N_{SW} by a m factor as well as the overall control complexity. The simplified matrix for the case of $m=3$ rows and $n=3$ solar modules per row is shown in Fig. 8a and b.

The PV modules current and voltage values were measured by a Data Acquisition system (DAQ) connected to a PC, which computed the controlling algorithm implemented in MATLAB. Table 1 shows the most relevant features of the Velasco et al. approach [84].

A variation of this technique was proposed in [90] as a mixed integer quadratic programming problem, which can be also applied when a non-equal number of modules per row is considered.

In [91] a particular switching matrix, named Dynamic Electrical Scheme (DES) shown in Fig. 9a, is proposed. It allows to implement two different reconfigurable controlling algorithms by computing the irradiance equalization. This solution creates rows with a non-equal number of modules, thus increasing the number of possible interconnection configurations. Calculation time, for a given number of modules, is fixed for the *deterministic search algorithm,* while in the *random search algorithm* it depends on the ending condition (e.g. prefixed number of iterations or flattening criterion). By the *deterministic search algorithm,* modules are ordered within the topology showed in Fig. 9b according to decreasing irradiance values. First, the minimum (N_{ROWmin}) and maximum (N_{ROWmax}) number of rows of the optimized PV array are set. The algorithm then looks for the optimal configuration starting with a number of rows (N_{Rows}) equal to N_{ROWmin}. The first N_{Rows} modules of the decreasing sequence are located one per row; then the remaining modules of the sequence are one by one connected to the row for which the sum of the irradiances of the modules already positioned is the minimum. After the last iteration, all modules are located and the total irradiations of rows are known. Then the algorithm calculates the equalization index by means of (9) and stores it. The number N_{Rows} is thus increased and the same procedure is repeated until $N_{Rows}=N_{ROWmax}$. Finally, the optimal configuration is the one that minimizes the equalization index.

The DES requires a number of switches N_{sw} equal to

$$N_{SW} = (2mN_{PV})_{DPST} + (m)_{SPDT} \tag{12}$$

Where DPST are double-pole single-throwswitches, N_{PV} is the number of PV modules and m is the number of rows, supporting up to$(m \cdot n)!/(n!)^m$ configurations.

Table 2 shows the most relevant features of the Candela et al. approach [91].

Another method based on the irradiance equalization principle was presented in [92]. The proposed technique is an iterative and hierarchical sorting algorithm, designed to achieve a near optimum configuration in an efficient way in terms of number of iterations. The irradiances of cells are obtained, arranged in descending order and mapped to the matrix of the physical PV array. Next, all even rows are flipped left to right and added to the preceding odd row, resulting in an averaged matrix. This method is applied again, resulting in a second average. The process stops when all the rows have been considered. A number of padding rows of zeros can be added if the number of rows is not a power of two nor an even number. An example is shown in Fig. 10. Although the proposed interconnection matrix supports each row having arbitrary number of modules, the algorithm enables to build rows having the same number of modules only. If single-pole single-throw (SPST) switches are used, the number of required switches, N_{sw}, is

$$N_{SW} = N_{PV} \cdot (m^2 - m) \tag{13}$$

where m is the number of rows.

Table 3 shows the most relevant features of the Wilson et al. approach [92].

In [93], a system architecture enabling the adaptive interconnection of solar cells inside a PV module was presented. This solution can be extended to a PV plant, where, instead of solar cells, many modules are considered. In this approach, a switching matrix connects a fixed number of fixed PV cells in a TCT topology, to another small reconfigurable (not fixed) bank of solar cells [76]. The number of switches required by this approach is smaller when compared to other solutions, for the presence of affixed part, thus enabling the use of simpler controlling algorithms. Under uniform irradiance conditions, static part and the adaptive one are connected together through the switching matrix shown in Fig. 11. If the first row is shaded, its voltage V_1 is less than a threshold voltage; otherwise, when the j-th row (with $j \neq 1$) is shaded, the output voltage is less than the quantity V_x:

$$V_{out} < V_x (\text{where } V_x = mV_1) \tag{14}$$

Where m is the number of rows. Both conditions trigger the reconfiguration phase. The logic of this approach relies on connecting the most irradiated cell of the bank (with the maximum open-circuit voltage) to the most shaded row of the fixed part, in order to compensate the irradiance (and thus the voltage) drop. A simple *bubble-sort* method and a quick *model-based* method are presented in [94] for controlling the switching matrix.

Table 4 shows the most relevant features of the Nguyen et al. approach [76].

In [95] a self-adaptive reconfiguration method based on fuzzy logic was proposed. When the voltage across a row is less than the threshold, the shading degree and the derivative of the irradiance are calculated, and then used as the inputs of a fuzzy controller. The latter calculates the number of PV cells of an adaptive bank needed to compensate the irradiance drop and then the reconfiguration is carried out.

Finally, In [96] the Su Do Ku puzzle pattern is used to physical arrange modules in a TCT connected PV array, distributing the shading effects over the array and consequently reducing the occurrence of shaded modules in the same row.

3.2. Reconfiguration in SP topology

Reconfiguration by means of SP topology aims to build strings of series-connected modules with similar irradiance levels and then connecting all these strings in parallel. In this way, well-irradiated solar panels will not be limited in current by a low irradiance panel of the same string.

A Flexible Switch array Matrix (FSM) was presented in [97]. The FSM is integrated with PV modules to form the Elastic Photovoltaic Structure (EPVS) as shown in Fig. 12. In uniform conditions, the PV system operates as a central inverter topology and the DC/DC converter is not used. When mismatch occurs, the proposed system excludes the shaded PV modules, reconfiguring the remaining ones in the main PV strings (MPV) and, if necessary, a sub-PV string (SPV). MPV strings have an equal number of modules connected directly to the inverter input, while SPV has fewer modules so that the DC/DC converter is used to connect this partial string to the inverter, thus avoiding mismatch losses. Four single-pole dual-throw (SPDT) switches are needed for every module, while two are required for the MPV bus and other two more for the SPV. The total number of required switches, N_{sw}, is given by the expression:

$$N_{sw} = (2N_{PV})_{SPDT} + (2N_{PV} + 4)_{SPST} \tag{15}$$

where N_{PV} is the number of modules and 4 are the switches required for the MPV and SPV bus. The identification of the irradiance conditions of PV modules was achieved by measuring voltage, current and temperature of each module. In [98] a 9-module prototype system implementing this approach is presented, showing power gains compatible with simulation results.

Table 5 shows the most relevant features of the Alahmad et al. approach [97].

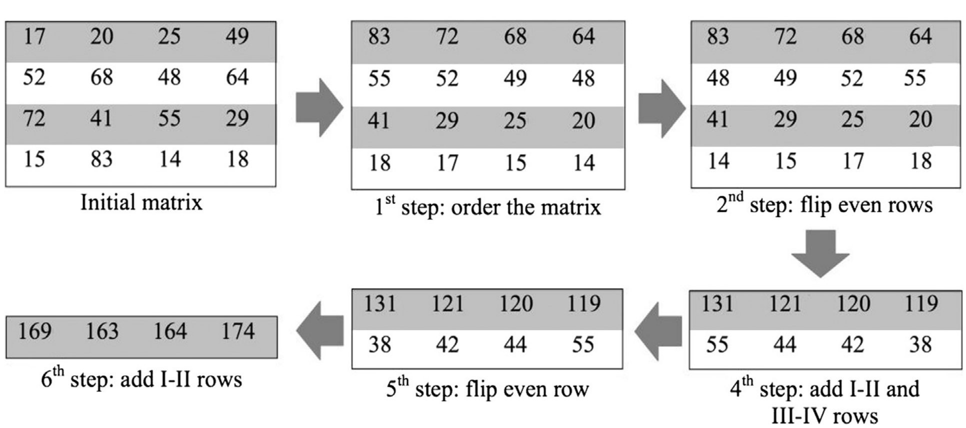


Fig. 10. Example of the best sorting algorithm.

Another approach using DC/DC converter is presented in [99], where multiple strings, each containing substrings of similar power levels only, were created. All the strings were connected to a DC/DC converter array, converging to a unique dc bus.

In [100]the aim was to build strings where solar cells having similar irradiance levels, G, are connected. The authors proposed three irradiance levels, based on different ranges: bright ($600 < G < 800\ W/m^2$), grey ($400 < G < 600\ W/m^2$) and dark ($G < 400\ W/m^2$) states as shown in Fig. 13. First, the current (I_b) across every bypass diode of each cell is sensed; when I_b is greater than zero the cell is dark, otherwise the short-circuit current (I_{sc}) is measured to classify the cell as bright or grey. The derivative of the short circuit current with respect to the time, indicated with dI_{sc}/dt, is evaluated, since grey cells can experience transitions towards dark or bright states. The sign of the I_{sc} derivative gives the direction of the transition [77] .

The proposed strategy calculates the number of shaded (dark) cells and if this is greater than 15% of the total, the reconfiguration occurs. Cells of the same state are combined in strings (bright strings and grey strings), while dark cells are excluded from the array, since their power contribution is negligible. The proposed system senses temperature and open-circuit voltage of each cell for monitoring purposes [101]. The proposed approach requires a number of switches N_{sw} equal to

$$N_{SW} = (m \cdot n) + \frac{((m \cdot n) - 1) \cdot (2 + (m \cdot n))}{2} \quad (16)$$

Table 6 shows the most relevant features of the Patnaik et al. approach [77].

Table 5
Summary of Alahmad et al. approach [97].

Reconfiguration strategy	Elastic photovoltaic structure
Control algorithm	–
Number of switches	$(2N_{PV})_{SPDT} + (2N_{PV} + 4)_{SPST}$
Acquired parameters	Voltage, current and temperature
Complexity and applicability	High

In [102] the Rough Set Theory (RST) is used to build an Automatic Reconfiguration System (ARS). For a SP topology of PV modules, different cases of shadowing conditions (when one or two modules are shaded) are considered and, for each of them, the most convenient SP connection of PV modules is selected. The RST helps to recognize similar or equivalent cases, producing simplified rules starting from the data of a decision table [103]. Each module of the PV array supplies a certain value of current $i(k)$. When $i(k)$ is less than a threshold current I_{ref} ($i(k) < I_{ref}$), the module is considered 'shaded'; on the contrary, if $i(k) > I_{ref}$ the module is considered 'unshaded'. For every module of the PV array, the information about its shading state is used by the set of rules and the correct rule is chosen. Every rule contains a switch configuration which sets the optimal configuration for the electrical connections of the panel. Table 7 shows the most relevant features of the Dos Santos et al. approach [98].

4. Challenging issues

4.1. Monitoring

A monitoring system for a PV array is usually needed to collect power production and performance data as well as weather conditions. This data enable to track the working conditions of each module, recognizing faulty solar panels, mismatch and partial shading conditions [104–107]. Monitored variables of interest are DC and AC electrical parameters (voltage, current, power), module and ambient temperature, irradiance, wind speed and humidity [108,109]. While the majority of monitoring systems collect data at a whole plant level, sensing parameters that are closer to each module are necessary when a PV module reconfiguration approach is adopted. As detailed in Section 2.3 and in the subsequent sections, most open loop control systems employed for dynamic reconfiguration purposes use the irradiance value since the irradiance equalization algorithm [110] requires the knowledge of the irradiance for every PV module. The most common method to sense the irradiance employs a pyranometer, thus common solar plants have one or few units for monitoring purpose. In order to have a good understanding of the spatial

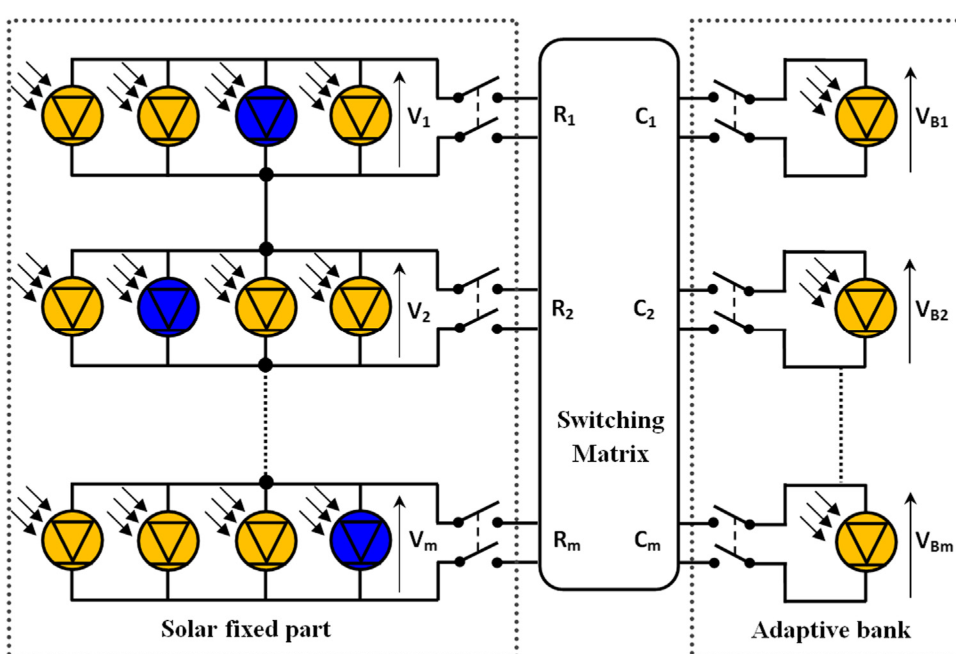


Fig. 11. Adaptive bank approach; the solar cells with low irradiance are blue-colored, while the yellow one are full irradiated.

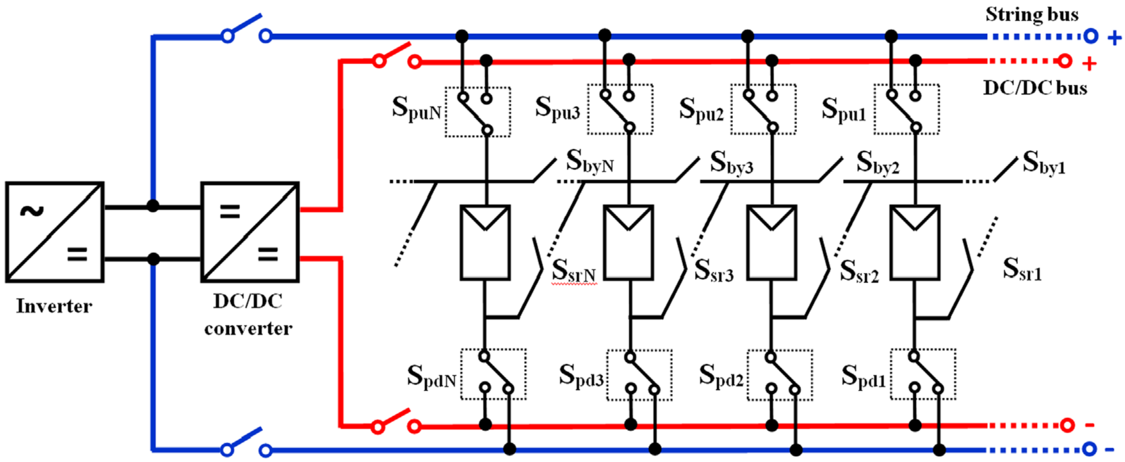


Fig. 12. Elastic Photovoltaic Structure (EPVS).

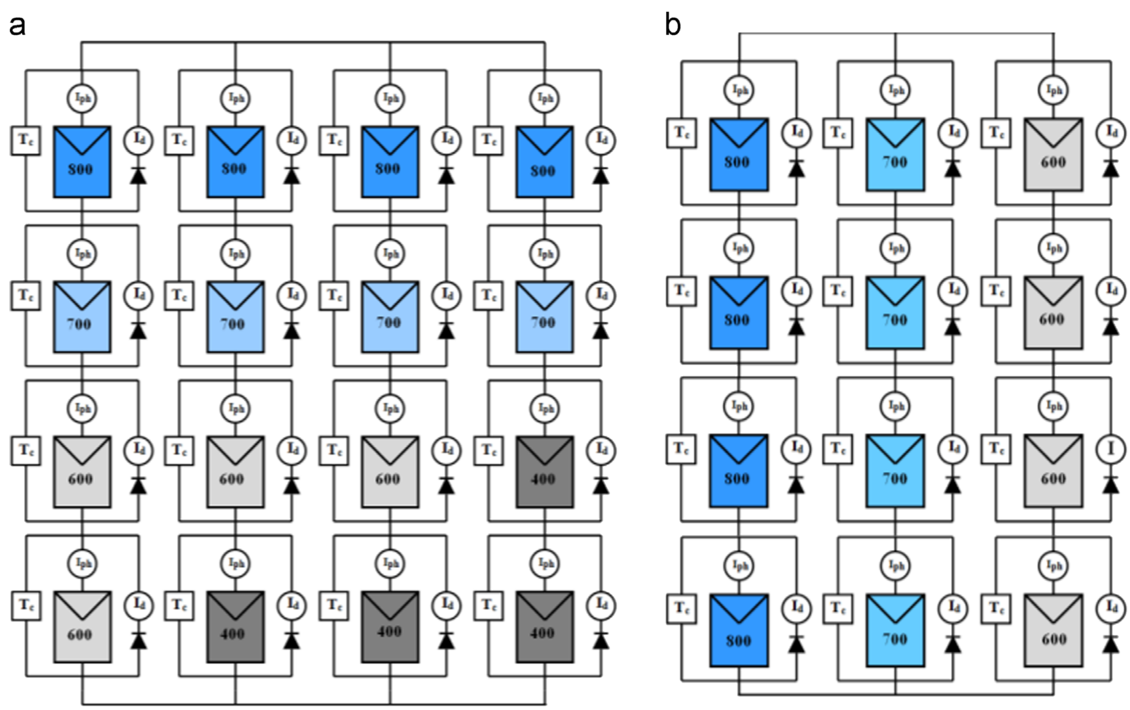


Fig. 13. Reconfiguration strategy in SP connection: (a) PV array with four different irradiance levels: 800, 700, 600 and 400 W/m^2, (b) after sorting, PV array is composed by three string with 800, 700 and 600 W/m^2. The PV panels with 400 W/m^2 are excluded.

Table 6
Summary of Patnaik et al. approach [77].

Reconfiguration strategy	Solar irradiance level categories
Control algorithm	–
Number of switches	$(mn+(mn-1)(2+mn))_{SPST}$
Acquired parameters	Cell temperature, bypass diode and short-circuit current
Complexity and applicability	Medium – High

Table 7
Summary of Dos Santos et al approach [102].

Reconfiguration strategy	Rough set theory
Control algorithm	Identification of optimal rule
Number of switches	Not-specified
Acquired parameters	Current
Complexity	Medium

irradiance profile, one pyranometer per PV module should be used, consequently increasing costs. Another approach estimates the irradiance level of each solar module by measuring the electrical characteristics of the modules. Voltage, current and temperature can be used in combination with the physical parameters of the given solar module to obtain the irradiance value using the PV electrical model in Eq. (5). In [89] and [97] a simplified model was used to estimate the irradiance, starting from the voltage and the current of the module. However in many real-world situations, temperature effects should not be neglected since, under shadow conditions, the temperature difference between modules can be significantly greater than zero. Thus, the irradiance levels can be considerably different even if modules have compatible values of voltage and current.

Table 8
Resume of the reconfiguration strategy in terms of: control algorithm, number of switch and acquiredparameters.

Authors	Strategy	Control algorithm	N° of switches	Acquired parameters	Complexity	Notes
TCT						
Velasco et al. [88]	Irradiance equalization	See control flow chart	$2N_{PV}m$-throws[a]	Row voltage and current of the module	Medium	Static and dynamic part
Romano et al. [91]	Irradiance equalization	Deterministic, Random-search	$(N_{PV})_{DPST}+m_{SPS}$	Irradiances	Medium	Supports rows with different number of modules
Wilson et al. [92]	Irradiance equalization	Best worst sorting	$N_{PV}(m^2-m)_{SPST}$	Voltage and current	Medium - High	Supports rows with different number of modules [b]
Nguyen et al. [76]	Adaptive bank	Bubble-sort, Model based	$(2N_{AB}N_{PV})_{SPST\ m}$[c]	Operating and open circuit voltage, temperature	Medium	Fixed part with an adaptive solar cells bank
SP						
Alahmad et al. [97]	EPVS	See control flow chart	$(2N_{PV})_{SPDT}+(2N_{PV}+4)_{SPST}$	Voltage, current e temperature	High	The string with the not-equal number of modules is matched by a DC/DC converter
Patnaik et al. [77]	Solar irradiance level categories	See control flow chart	$(mn+(mn-1)(2+mn))_{SPST}$[d]	Cell temperature, bypass diode current and short-circuit current	Medium - High	Irradiance classified in bright, grey and dark levels
Dos Santos et al. [102]	Rough set theory	Identification of optimal rule	Not specified	Current	Medium	Simplified logic rules to select optimal switch configuration

[a] This can be reduced and the switching matrix simplified.
[b] The algorithm enables only to build rows having the same number of modules, despite the interconnection matrix is more flexible.
[c] N_{AB} number of adaptive banks.
[d] *m, n* number of rows and columns respectively.

It is worth mentioning that, while in a SP topology it is necessary to acquire the voltage for each module but only the current of each string, in a TCT topology the voltage of every row and the current of each module are needed. Thus in a TCT topology more current sensors are used. Another approach relies on short-circuit current sensing of each module, estimating G by Eq.(7). The advantage of this method is that I_{sc} has a linear dependence on irradiance [77] and also is not very sensitive to temperature variations, thus temperature measurements are not necessary. This approach however requires each solar module to be electrically disconnected from the PV array and to be short-circuited for every measurement, not only causing lack of its power contribution, but even leading to the stop of the inverter MPPT algorithm if the minimum voltage and current input ranges are not satisfied due to its exclusion. In order to avoid installing current sensors, usually more expensive than voltage sensors, the open-circuit voltage V_{oc} and the temperature of each module can be measured and G estimated by using (4). Even in this case, each solar module will be electrically disconnected from the PV array. In [76] a similar approach was used to evaluate irradiance levels, although the temperature is not acquired for each module.

Monitoring a fixed PV plant in order to evaluate the affordability of its conversion to a reconfigurable plant is an issue of great interest. For such application, a wireless monitoring system [111] could be adopted for sensing the electrical characteristics of each module of the plant, thus processing the acquired data to evaluate the power improvement that could be obtained using a reconfigurable interconnection matrix.

4.2. Switching matrix

The switching matrix is one of the most crucial points of a dynamic PV reconfiguration system. The switching architecture must provide strong reliability, low costs, low maintenance and its life-time should be the same of the PV generator itself. Different kinds of switches exist and these include mechanical or solid-state relays, contactors, MOSFETs, IGBTs, SCRs. MOSFETs are interesting because of their relative low cost, high efficiency and high power availability but their control can be difficult. A solution based on MOSFETs was presented in [101] [112]. Relays are in many cases the most effective choice, mainly in the mechanical version. In fact, although solid-state relays offer a higher cycles lifetime because they have no moving parts, they are more expensive for the higher currents needed by PV module interconnections. Since switching matrix costs are proportional to the number of relays and their costs are nearly proportional to rated current, solutions minimizing the number of switches and topologies where current through relays is lower, should be adopted.

It is interesting to observe that the number of required switches influence the fixed installation costs while the number of switching operations influences the lifetime of the entire apparatus and thus can be considered as variable operating costs, although in the literature there is not a deep insight about this issue.

Latching relays can be very convenient since they need a driver only when it is necessary to switch contacts, so that they consume nearly zero static power. Also, the driver circuit can be multiplexed to many or all the relays, depending if it is desired switching many relays at the same time or one by one sequentially. Some authors, for instance [88] and [102] presented switching matrixes requiring one-pole to multiple-throws relays. Since commercial off-the-shelf relays provide a limited number of multiple-throws, these must be emulated by connecting many single pole relays in parallel, thus increasing overall control complexity as well as costs.

5. Summary and discussion

In this paper, some of the most interesting PV reconfiguration strategies for different PV plant topologies presented in the literature have been discussed. While many commercial solutions rely on the classic Series Parallel topology, the Total Cross Tied topology has raised a great interest from many authors. TCT offers effective optimization algorithms and higher flexibility, see Table 8, despite the higher currents of this topology usually lead to more expensive cabling, thus reducing the Return-on-Investments (ROI) index. Furthermore, for small PV plants the overall voltage plant output is less than in the case of the SP topology.

On the other hand, marketing target in the next years, could be the conversion of fixed PV plants into reconfigurable ones; in this way, keeping the SP topology will save re-designing efforts and costs. Adding a dynamic reconfiguration system to an existing PV plant that benefits from a particular feed in tariff would produce not only an increase of the energy produced but also an increase of the economic advantages connected to the relevant feed in tariff.

Under the “ContoEnergia V” promoted by the Italian government in the 2012, the installation of a power optimizer device such as a dynamic reconfiguration system would be rewarded with a further economic incentive in the €/MWh-produced tariff to the owner of the plant that could reach 1.38 the original reward.

For this market, monitoring a fixed PV plant for a certain period could be of a great interest in order to evaluate the conversion feasibility.

Nonetheless, it could be possible to design a reconfigurable interconnection device supporting both SP and TCT interconnection topologies at the same time, but on the other hand, many switches would be needed and, as a result, costs would be increased. Therefore, the interconnection topology should be chosen first. While it could be possible to address the TCT connection topology for new plant designs and the SP for the conversion of existing plants, a better comparison study on the TCT versus SP reconfigurable approach should be needed in terms of investments, reliability and power improvements. The overall complexity of the solution and total cost are indeed important factors to evaluate a proper reconfigurable approach. Table 8 provides an overview of the reconfiguration strategies discussed in this paper. Further research on the topic should be addressed towards the definition of efficient switching matrices also taking into account the lifetime of switches, not only installation costs, as well as the identification of applicability issues for each considered strategy.

Acknowledgements

This work has been funded by MIUR by means of the national Program PON R&C 2007–2013, ENERGETIC PON02_00355_3391233 2012-2014.

References

[1] Fischer C, Preonas L. Combining policies for renewable energy: is the whole less than the sum of its parts. Int Rev Environ Resource Econom 2010;4(1):51–92.
[2] Solangi K, Islam M, Saidur R, Rahim N, Fayaz H. A review on global solar energy policy. Renew Sustain Energy Rev 2011;15(4):2149–63.
[3] Zhang P, Li W, Li S, Wang Y, Xiao W. Reliability assessment of photovoltaic power systems: review of current status and future perspectives. Appl Energy 2013;104:822–33.
[4] Green MA, Emery K, Hishikawa Y, Warta W, Dunlop ED. Solar cell efficiency tables. Prog Photovolt: Res Appl 2012;20(1):12–20.
[5] Meral ME, Dinçer F. A review of the factors affecting operation and efficiency of photovoltaic based electricity generation systems. Renew Sustain Energy Rev 2011;15(5):2176–84.
[6] Di Dio V, La Cascia D, Miceli R., Rando C. A mathematical model to determine the electrical energy production in photovoltaic fields under mismatch effect pp. 46–51, 2009.
[7] Abdalla IA. Integrated PV and multilevel converter system for maximum power generation under partial shading conditions; 2013, (PhD thesis), 〈http://etheses.whiterose.ac.uk/4603/1/Thesis2013.pdf〉.
[8] Parida B, Iniyan S, Goic R. A review of solar photovoltaic technologies. Renew Sustain Energy Rev 2011;15(3):1625–36.
[9] Singh G. Solar power generation by PV (photovoltaic) technology: a review. Energy 2013.
[10] Razykov T, Ferekides C, Morel D, Stefanakos E, Ullal H, Upadhyaya H. "Solar photovoltaic electricity: current status and future prospects. Sol Energy 2011;85(8):1580–608.
[11] Makrides G, Zinsser B, Norton M, Georghiou GE, Schubert M, Werner JH. Potential of photovoltaic systems in countries with high solar irradiation. Renew Sustain Energy Rev 2010;14(2):754–62.
[12] Bhatnagar P, Nema R. Maximum power point tracking control techniques: state-of-the-art in photovoltaic applications. Renew Sustain Energy Rev 2013;23:224–41.
[13] Ishaque K, Salam Z. A review of maximum power point tracking techniques of PV system for uniform insolation and partial shading condition. Renew Sustain Energy Rev 2013;19:475–88.
[14] Reza Reisi A, Hassan Moradi M, Jamasb S. Classification and comparison of maximum power point tracking techniques for photovoltaic system: a review. Renew Sustain Energy Rev 2013;19:433–43.
[15] Mousazadeh H, Keyhani A, Javadi A, Mobli H, Abrinia K, Sharifi A. A review of principle and sun-tracking methods for maximizing solar systems output. Renew Sustain Energy Rev 2009;13(8):1800–18.
[16] Chao K-H, Ho S-H, Wang M-H. Modeling and fault diagnosis of a photovoltaic system. Electr Power Syst Res 2008;78(1):97–105 (January).
[17] Hirata Y, Noro S, Aoki T, Miyazawa S. Diagnosis photovoltaic failure by simple function method to acquire I-V curve of photovoltaic modules string, pp. 10–13, 2011.
[18] Deline C, Dobos A, Janzou S, Meydbray J, Donovan M. A simplified model of uniform shading in large photovoltaic arrays. Sol Energy 2013;96:274–82.
[19] García MC, Herrmann W, W., Böhmer PB. Thermal and electrical effects caused by outdoor hot-spot testing in associations of photovoltaic cells. Prog Photovolt: Res Appl 2003;11(5):293–307.
[20] Giaffreda D, Omana M, Rossi D., Metra C., Model for thermal behavior of shaded photovoltaic cells under hot-spot condition. In: Defect and fault tolerance in VLSI and nanotechnology systems (DFT), 2011 IEEE international symposium on, 2011.
[21] Spagnolo GS, Del Vecchio P, Makary G, Papalillo D, Martocchia A. A review of IR thermography applied to PV systems. In: Environment and electrical engineering (EEEIC). In: 2012 Eleventh international conference on, 2012.
[22] Herrmann W, Wiesner W, Vaassen W. Hot spot investigations on PV modules-new concepts for a test standard and consequences for module design with respect to bypass diodes. In: Photovoltaic specialists conference, 1997., conference record of the twenty-sixth IEEE, 1997.
[23] Meyer EL, van Dyk EE. Assessing the reliability and degradation of photovoltaic module performance parameters. Reliab, IEEE Trans 2004;53(1):83–92.
[24] Candela R, di Dio V, Sanseverino ER and Romano P Reconfiguration techniques of partial shaded PV systems for the maximization of electrical energy production. In: 2007 International conference on clean electrical power; 2007. p. 716–9.
[25] Silvestre S, Boronat a, Chouder a. Study of bypass diodes configuration on PV modules. Appl Energy 2009;86(9):1632–40.
[26] Gokmen N, Karatepe E, Ugranli F, Silvestre S. Voltage band based global MPPT controller for photovoltaic systems. Sol Energy 2013;98:322–34.
[27] Bouilouta A, Mellit A, Kalogirou S. New MPPT method for standalone photovoltaic systems operating under partially shaded conditions. Energy 2013.
[28] Alajmi BN, Ahmed KH, Finney SJ, Williams BW. A maximum power point tracking technique for partially shaded photovoltaic systems in microgrids. IEEE Trans Ind Electron 2013;60(4):1596–606.
[29] Ji Y-H, Jung D-Y, Kim J-G, Kim J-H, Lee T-W, Won C-Y. A real maximum power point tracking method for mismatching compensation in PV array under partially shaded conditions. Power Electron, IEEE Trans 2011;26(4):1001–9.
[30] Koutroulis E, Blaabjerg F. A new technique for tracking the global maximum power point of PV arrays operating under partial-shading conditions. Photovolt, IEEE J 2012;2(2):184–90.
[31] Poshtkouhi S, Biswas A and Trescases O. DC-DC converter for high granularity, sub-string MPPT in photovoltaic applications using a virtualparallel connection. In: Applied power electronics conference and exposition (APEC), 2012 twenty-seventh annual IEEE, 2012.
[32] Poshtkouhi S, Palaniappan V, Fard M, Trescases O. A general approach for quantifying the benefit of distributed power electronics for fine grained MPPT in photovoltaic applications using 3-D modeling. Power Electron, IEEE Trans 2012;27(11):4656–66.
[33] Obane H , Okajima K, Ozeki T, Yamada T, Ishi T, Corporation E. Minimizing mismatch loss in bipv system by reconnection, pp. 2406–11, 2011.
[34] Obane H, Member S, Okajima K, Oozeki T. PV System with reconnection to improve output under nonuniform illumination 2012;2(3):341–7.
[35] Maki A, Valkealahti S. Power losses in long string and parallelconnected short strings of series-connected silicon-based photovoltaic modules due to partial shading conditions. Energy Convers, IEEE Trans 2012;27(1):173–83.
[36] Ramos-Paja C, Bastidas J, Saavedra-Montes A, Guinjoan-Gispert F, Goez M. "Mathematical model of total cross-tied photovoltaic arrays in mismatching conditions. In: Circuits and systems (CWCAS), 2012 IEEE fourth Colombian workshop on; 2012.
[37] Zhao Y, Yang L, Lehman B, de Palma J, Mosesian J, Lyons R. Decision tree-based fault detection and classification in solar photovoltaic arrays. In: Applied power electronics conference and exposition (APEC), 2012 twenty-seventh annual IEEE; 2012.
[38] Skoplaki E, Palyvos J. On the temperature dependence of photovoltaic module electrical performance: a review of efficiency/power correlations. Sol Energy 2009;83(5):614–24.
[39] Martínez-Moreno F, Muñoz J, Lorenzo E. Experimental model to estimate shading losses on PV arrays. Sol Energy Mater Sol Cells 2010;94(12):2298–303.

[40] de Oliveira Reiter RD, Michels L, Pinheiro JR, Reiter RA, Oliveira SVG, Peres A. Comparative analysis of series and parallel photovoltaic arrays under partial shading conditions. In: Industry applications (INDUSCON), 2012 tenth IEEE/IAS international conference on; 2012.
[41] Alonso-Garcia M, Ruiz J. Analysis and modelling the reverse characteristic of photovoltaic cells. Sol Energy Mater Sol Cells 2006;90(7):1105–20.
[42] Karatepe E, Boztepe M, Colak M. Development of a suitable model for characterizing photovoltaic arrays with shaded solar cells. Sol Energy 2007;81(8):977–92.
[43] Tian H, Mancilla-David F, Ellis K, Muljadi E, Jenkins P. Determination of the optimal configuration for a photovoltaic array depending on the shading condition. Sol Energy 2013;95:1–12.
[44] Mermoud A, Lejeune T. Partial shadings on pv arrays: by-pass diode benefits analysis. In: Proceedings of the twenty-fifth European photovoltaic solar energy conference, Valencia, Spain, 2010.
[45] Patel H, Agarwal V, Member S. MATLAB-based modeling to study the effects of partial shading on PV array characteristics 2008;23(1):302–10.
[46] Villalva MG, Gazoli JR. "Comprehensive approach to modeling and simulation of photovoltaic arrays. Power Electronics, IEEE Transactions on 2009;24 (5):1198–208.
[47] Storey J, Wilson PR, Bagnall D. Simulation platform for dynamic photovoltaic arrays, in Energy Conversion Congress and Exposition (ECCE), 2013 IEEE, 2013.
[48] Myrzik J, Calais. String and module integrated inverters for singlephase grid connected photovoltaic systems-a review. In: Power tech conference proceedings, 2003 IEEE Bologna, 2003.
[49] Elasser A, Agamy M, Sabate J, Steigerwald R, Fisher R, Todorovic M. Harfman-A comparative study of central and distributed MPPT architectures for megawatt utility and large scale commercial photovoltaic plants. In: IECON 2010-thirty-sixth annual conference on IEEE industrial electronics society, 2010.
[50] Bo Y, Xu Y, Donghao L, Zhaoan W. A new architecture for high efficiency maximum power point tracking in grid-connected photovoltaic system. In: Power electronics and motion control conference, 2009. IPEMC'09. IEEE sixth international, 2009.
[51] Li Q, Wolfs P. A review of the single phase photovoltaic module integrated converter topologies with three different DC link configurations. Power Electron, IEEE Trans 2008;23(3):1320–33.
[52] O'Callaghan L, McKeever M, Norton B. A simulation analysis of photovoltaic AC module integrated converters in parallel, under controlled edge shading conditions. In: Environment and electrical engineering (EEEIC), 2012 eleventh international conference on, 2012.
[53] Tsao P, Sarhan S, Jorio I. Distributed max power point tracking for photovoltaic arrays. In: Photovoltaic specialists conference (PVSC), 2009 thirty-fourth IEEE; 2009.
[54] Kjaer SB, Pedersen JK, Blaabjerg F. A review of single-phase gridconnected inverters for photovoltaic modules. Ind Appl, IEEE Trans 2005;41 (5):1292–306.
[55] Townsend TU. A method for estimating the long-term performance of direct-coupled photovoltaic systems; 1989.
[56] Bouzguenda M, Salmi T, Gastli A, Masmoudi A. Evaluating solar photovoltaic system performance using MATLAB. In: Renewable energies and vehicular technology (REVET), 2012 first international conference on, 2012.
[57] Lo Brano V, Orioli A, Ciulla G. On the experimental validation of animproved five-parameter model for silicon photovoltaic modules. Sol Energy Mater Sol Cells 2012;105:27–39.
[58] Wolf M, Rauschenbach H. Series resistance effects on solar cell measurements. Adv Energy Convers 1963;3(2):455–79.
[59] Luque A, Hegedus S. Handbook of photovoltaic science and engineering. Wiley; 2011.
[60] Ortiz-Conde A, Garcìa Sanchez FJ, Muci J. New method to extract the model parameters of solar cells from the explicit analytic solutions of their illuminated I-V characteristics. Sol Energy Mater Sol Cells 2006;90 (3):352–61.
[61] Salmi T, Bouzguenda M, Gastli A, Masmoudi A. MATLAB/Simulink based modeling of photovoltaic cell. Int J Renew Energy Res (IJRER) 2012;2 (2):213–8.
[62] Farivar G, Asaei B. Photovoltaic module single diode model parameters extraction based on manufacturer datasheet parameters. In: Power and energy (PECon), 2010 IEEE international conference on; 2010.
[63] Ishaque K, Salam Z, Taheri H. Simple, fast and accurate two-diode model for photovoltaic modules. Sol Energy Mater Sol Cells 2011;95(2):586–94.
[64] Cipriani G, Di Dio V, La Cascia D, Miceli R, Rizzo R. A novel approach for parameters determination in four lumped PV parametric model with operative range evaluations. Int Rev Electr Eng (I.R.E.E.) 2013;8(3):1827–-6660 (ISSN).
[65] Kadri R, Andrei H, Gaubert J-P, Ivanovici T, Champenois G, Andrei P. Modeling of the photovoltaic cell circuit parameters for optimum connection model and real-time emulator with partial shadow conditions. Energy 2012;42(1):57–67.
[66] Ishaque K, Salam Z, Taheri H. Modeling and simulation of photovoltaic (PV) system during partial shading based on a two-diode model. Simul Modell Pract Theory 2011;19(7):1613–26.
[67] Celik AN, Acikgoz N. Modelling and experimental verification of the operating current of mono-crystalline photovoltaic modules using fourand five-parameter models. Appl Energy 2007;84(1):1–15.
[68] juen Wang Y, chun Hsu P. Analysis of partially shaded PV modules using piecewise linear parallel branches model 2009:783–9.
[69] De Soto W, Klein S, Beckman W. Improvement and validation of a model for photovoltaic array performance. Sol Energy 2006;80(1):78–88.
[70] Dunford W, Capel A. A novel modeling method for photovoltaic cells. In: 2004 IEEE thirty-fifth annual power electronics specialists conference (IEEE Cat. No.04CH37551); 2004. p. 1950–6.
[71] Carrero C, Amador J, Arnaltes S. A single procedure for helping PV designers to select silicon PV modules and evaluate the loss resistances. Renew Energy 2007;32(15):2579–89.
[72] Liu S, Dougal RA. Dynamic multiphysics model for solar array. Energy Convers, IEEE Trans 2002;17(2):285–94.
[73] Lo Brano V, Orioli A, Ciulla G, Di Gangi A. An improved fiveparameter model for photovoltaic modules. Sol Energy Mater Sol Cells 2010;94(8):1358–70.
[74] Yadir S, Benhmida M, Sidki , Assaid E and Khaidar M. New method for extracting the model physical parameters of solar cells using explicit analytic solutions of current-voltage equation. In: Microelectronics (ICM), 2009 international conference on; 2009.
[75] Sera D, Teodorescu R and Rodriguez P. PV panel model based on datasheet values. In: Industrial electronics, 2007. ISIE 2007. IEEE international symposium on; 2007.
[76] Nguyen D, Lehman B. An adaptive solar photovoltaic array using model-based reconfiguration algorithm. IEEE Trans Ind Electron 2008;55(7): 2644–2654.
[77] Patnaik B. Distributed multi-sensor network for real time monitoring of illumination states for a reconfigurable solar photovoltaic array," Phys. Technol Sens (ISPTS), 2012.
[78] Ramaprabha R, Mathur BL. A comprehensive review and analysis of solar photovoltaic array configurations under partial shaded conditions. Int J Photoenergy 2012:1–16.
[79] Ramabadran R. Effect of shading on series and parallel connected solar PV modules. Modern Appl Sci 3(10).
[80] Ramaprabha R, Mathur B, Murthy M, Madhumitha S. New configuration of solar photo voltaic array to address partial shaded conditions. In: 2010 third international conference on emerging trends in engineering and technology, p. 328–333, 2010.
[81] Ramaprabha R, Mathur B. Modelling and simulation of Solar PV Array under partial shaded conditions. In: 2008 IEEE international conference on sustainable energy technologies; 2008. p. 7–11.
[82] Picault D, Raison B, Bacha S, Aguilera J, De La Casa J. Changing photovoltaic array interconnections to reduce mismatch losses: a case study. In: IEEE conference publications; May 2010.
[83] El-dein MZS, Member S, Kazerani M, Member S. "Novel configurations for photovoltaic farms to reduce partial shading losses, pp. 1–5, 2011.
[84] Villa LF L, Picault D, Raison B, Bacha S, Labonne A. Maximizing the power output of partially shaded photovoltaic plants through optimization of the interconnections among its modules. Photovolt, IEEE J 2012;2(2):154–63.
[85] Roopa P, Rajan S and Vengatesh R. Performance analysis of PV module connected in various configurations under uniform and non-uniform solar radiation conditions. In: Recent advancements in electrical, electronics and control engineering (ICONRAEeCE), 2011 International conference on; 2011.
[86] Gao L, Dougal RA, Liu S, Iotova AP. Parallel-connected solar PV system to address partial and rapidly fluctuating shadow conditions. Ind Electron, IEEE Trans 2009;56(5):1548–56.
[87] Picault D, Raison B, Bacha S, De La Casa J, Aguilera J, Casa JD L, et al. Forecasting photovoltaic array power production subject to mismatch losses. Sol Energy 2010;84(7):1301–9.
[88] Velasco-Quesada G, Guinjoan-Gispert F, Piquè-Lopez R, Romàn- Lumbreras M, Conesa-Roca A. Electrical PV array reconfiguration strategy for energy extraction improvement in grid-connected PV systems 2009;56 (11):4319–31.
[89] Velasco G, Negroni JJ, Guinjoan F, Pique R. Energy generation in PV grid-connected systems : power extraction optimization for plant oriented PV generators 2005:1025–30.
[90] El-Dein MS, Kazerani M, Salama M. Optimal total cross tied interconnection for reducing mismatch losses in photovoltaic arrays 2012:1–9 (ieeexplore.ieee.org).
[91] Romano P, Candela R, Cardinale M, Li Vigni V, Musso D, Sanseverino E Riva. Optimization of photovoltaic energy production through an efficient switching matrix. J Sustain Dev Energy, Water Environ Syst 2013;1(3):227–36.
[92] Wilson P, Storey J, Bagnall D. Improved optimization strategy for irradiance equalization in dynamic photovoltaic arrays. IEEE Trans Power Electron 2013;28(6):2946–56.
[93] Nguyen DD, Lehman B. Performance evaluation of solar photovoltaic arrays including shadow effects using neural network IEEE energy conversion congress and exposition, pp. 3357–62, 2009.
[94] Nguyen D, Lehman B. Modeling and simulation of solar PV arrays under changing illumination conditions 2006 IEEE workshops on computers in power electronics, pp. 295–99, 2006.
[95] Cheng Z, Pang Z, Liu Y, Xue P. An adaptive solar photovoltaic array reconfiguration method based on fuzzy control 2010 Eighth World Congress on intelligent control and automation, pp. 176–81, 2010.
[96] Rani BI, Ilango GS, Nagamani C. Enhanced power generation from PV array under partial shading conditions by shade dispersion using Su Do Ku configuration; 2012.

[97] Alahmad M, Chaaban MA, Lau SK, Shi J, Neal J. An adaptive utility interactive photovoltaic system based on a flexible switch matrix to optimize performance in real-time. Sol Energy 2012;86(3):951–63 (March).
[98] Chaaban MA, Alahmad M, J Neal, Shi J, Berryman C, Cho Y., et al. Adaptive photovoltaic system. IECON 2010 – thirty-sixth annual conference on IEEE industrial electronics society; November 2010. p. 3192–7.
[99] Storey J, Wilson PR, Bagnall D. The optimized string dynamic photovoltaic array, IEEE Trans Power Electron, 2013.
[100] Patnaik B, Sharma P, Trimurthulu E, Duttagupta SP, Agarwal V. Reconfiguration strategy for optimization of solar photovoltaic array under non-uniform illumination conditions. In: 2011 Thirty-seventh IEEE photovoltaic specialists conference; June 2011. p. 1859–64.
[101] Patnaik B, Mohod J, Duttagupta SP. Dynamic loss comparison between fixed-state and reconfigurable solar photovoltaic array 2011:1633–8.
[102] dos Santos P, Vicente EM, Ribeiro ER. Reconfiguration methodology of shaded photovoltaic panels to maximize the produced energy. In: XI Brazilian power electronics conference; September 2011. p. 700–706.
[103] dos Santos P, Vicente E. M., Ribeiro ER. Relationship between the shading position and the output power of a photovoltaic panel. In: XI Brazilian Power Electronics Conference; September 2011. p. 676–81.
[104] Firth S, Lomas K, Rees S. A simple model of PV system performance and its use in fault detection. Sol Energy 2010;84(4):624–35 (April).
[105] Oozeki T, Izawa T, Otani K, Kurokawa K. An evaluation method of PV systems. Sol Energy Mater Sol Cells 2003;75(3–4):687–95.
[106] Benghanem M, Maafi A. Data acquisition system for photovoltaic 1998;47 (1):30–3.
[107] Zou X, Bian L, Yonghui Z, Haitao L, Description A, Pv G-c. Performance monitoring and test system for grid-connected photovoltaic systems 2012:1–4.
[108] Commission IE. International standard IEC 61724: photovoltaic system performance. IEC 1998.
[109] van Dyk E, Meyer E, Vorster F, Leitch a. Long-term monitoring of photovoltaic devices. Renew Energy 2002;25(2):183–97.
[110] Velasco G, Negroni J. Irradiance equalization method for output power optimization in plant oriented grid-connected PV generators. Power Electron Appl 2005.
[111] Xiaoli X, Daoe Q. Remote monitoring and control of photovoltaic system using wireless sensor network. In: 2011 International conference on electric information and control engineering; April 2011. p. 633–8.
[112] Tria LA R, Escoto MT, Odulio CM F. Photovoltaic array reconfiguration for maximum power transfer. TENCON 2009 – 2009 IEEE region 10 conference 2009:1–6.